

AN EXPERIMENTAL STUDY OF THE PRACTICAL STABILITY OF SOLUTIONS OF ORDINARY DIFFERENTIAL EQUATIONS*

by

JACEK OLSZEWSKI and WŁADYSŁAW TURSKI

Introduction

This paper is concerned with the description of certain experiments carried out on high speed computers and intended to explore the practical possibility of realizing digital models for learning automata in control of dynamic processes. We shall call a dynamic process any physical phenomenon the description of which can be presented in the form of the set of solutions of a normal system of ordinary differential equations. Of all the possible problems in controlling the course of dynamic processes we shall select the simplest and probably the most important one, viz., determining whether, if the process is at the given point of the phase space at the given moment of time, its development, during the immediately following time units T , will be satisfactory even though the process will be influenced by unknown (but small) perturbing factors. The ability of finding quick answers to this question plays a major role in any decision taking process.

1. Geometrical Principles of the Algorithm Simulating the Learning Automaton

It has been suggested in the papers [1] and [2] that a digital model of the heuristic automaton endowed with "learning" ability, be used to solve the problem stated in the introduction. In this chapter we are going to present an outline of the geometrical principles of the operation of such a model. The model subjected to the experiments to be described was realized on the digital computer Ural-2 by the algorithm differing in certain details from that presented in the appendix to the paper [2].

*The paper was submitted on 1. X. 1964.

In this chapter the operation of the model will be presented as applied to the following system of equations:

$$\begin{aligned}\frac{dx_1}{dt} &= -x_2 + A \sin \omega t, \\ \frac{dx_2}{dt} &= x_1 + A \cos \omega t, \quad \omega \neq -1,\end{aligned}\tag{1.1}$$

where A and ω are real numbers.

The system has the following solution:

$$\begin{aligned}x_1 &= \left[C_1 \cos t + C_2 \sin t - \frac{A}{\omega + 1} \right] \cos \omega t, \\ x_2 &= \left[-C_2 \cos t + C_1 \sin t + \frac{A}{\omega + 1} \right] \sin \omega t,\end{aligned}\tag{1.2}$$

where the constants C_1 and C_2 are determined by the initial conditions:

$$\begin{aligned}C_1 &= x_1^0 + \frac{A}{\omega + 1}, \\ C_2 &= -x_2^0\end{aligned}$$

Let us pose the question:

What is the set of the initial conditions X , such that for every $(x_1^0, x_2^0) \in X$ there holds $(x_1(t), x_2(t)) \in K$ for $t \in [0, T]$, if K is a circle with radius R and center $(0, 0)$.

Since the solutions (1.2) are periodic functions with the period

$$\tau = \frac{2\pi}{\omega},$$

we select T so that: $T = \tau$.

By denoting: $r^2(t) = x_1^2(t) + x_2^2(t)$ we obtain:

$$r^2(t) = C_1^2 + C_2^2 + \left(\frac{A}{\omega + 1} \right)^2 - 2 \frac{A}{\omega + 1} \sqrt{C_1^2 + C_2^2} \sin[(\omega + 1)t + \varphi],$$

where the phase shift, φ , is a variable independent of t . As is easily seen:

$$\max_{0 \leq t \leq T} (r^2(t)) = \left(\sqrt{C_1^2 + C_2^2} + \frac{A}{\omega + 1} \right)^2.$$

From the above it follows that for the solutions not to leave K within the time T it is necessary and sufficient that the initial conditions belong to the circle with center $\left(-\frac{A}{\omega + 1}, 0 \right)$ and the radius equal to $R - \frac{A}{\omega + 1}$. In the example chosen for the experiments with the automaton model it was assumed that: $\omega = 0.5$, $A = 3$, $R = 5$.

The operation of the model begins with the random choice¹ of the coordinates of the point $P_1 \in K'$, where K' is a square circumscribed about K . For technical reasons the random choosing of points from the square was much faster than that from the circle.

Having chosen at random the point P_1 (and all the following points P_j) we determine, by means of the numerical integration of equations (1.1) with the initial conditions: $x_1(0) = x_{1j}$, $x_2(0) = x_{2j}$, where $(x_{1j}, x_{2j}) = P_j$, employing the method of Runge-Kutta-Gill [3], the binary function $\Sigma(P)$ such that

$$\Sigma(P_j) = \begin{cases} 0 & \text{for } P_j \text{ such that } (x_1(t), x_2(t)) \in K \text{ for } t \in [0, T], \\ 1 & \text{for } P_j \text{ such that there exists such } \vartheta \in [0, T], \text{ that } (x_1(\vartheta), x_2(\vartheta)) \notin K. \end{cases}$$

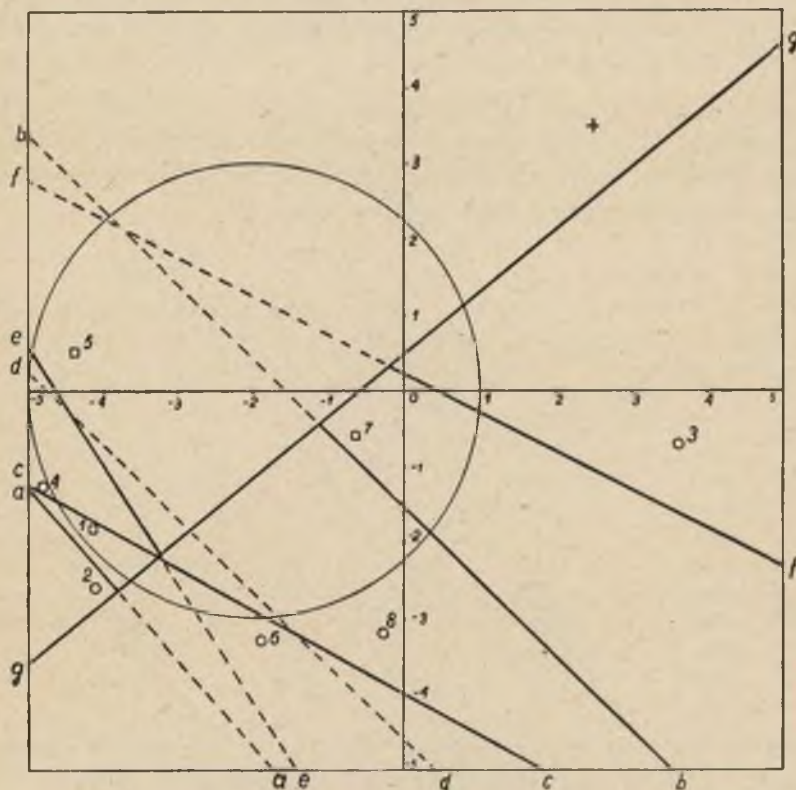


Fig. 1. Figures formed by the automaton model for $S = 7$

□ — the points for which $\Sigma(P) = 0$, ○ — the points for which $\Sigma(P) = 1$,
 - - - - the lines and the line segments which were removed during the learning process, + — the test point, the set X is denoted by the circle

¹ In all random selections the J. Banasiewicz's subroutine generating pseudo-random numbers uniformly distributed in the interval $[-1, 1]$ was applied. The subroutine is based on the principle presented by G. Neovius in "Ericsson Techniques", 1955, No. 2, p. 280.

Then we choose at random the sequence of points P_{2_i} until we obtain $\Sigma(P_{2_N}) = 1 - \Sigma(P_1)$, following which we assume: $P_2 = P_{2_N}$.

The coordinates of the randomly chosen points are placed in Table 1, and the points themselves are in Fig. 1 where the squares indicate the points for which $\Sigma(P) = 0$, and the circles indicate those for which $\Sigma(P) = 1$. Having chosen at random the points P_1 and P_2 we run the line aa between them. The coefficients of the line:

$$ux_1 + vx_2 = w$$

are determined in the following way: the numbers u and v are drawn at random from the interval $[-1, 1]$, while:

$$w = \frac{1}{2} [u(x_{11} + x_{12}) + v(x_{21} + x_{22})].$$

It has been pointed out by J. Łukaszewicz, to whom we are grateful for this remark, that this choice of coefficients introduces undesirable anisotropy. Thus in future applications it would be better to choose (u, v) from unit circle rather than from unit square.

Table 1

The coordinates of the randomly chosen points

No.	x_1	x_2
1	-4.15	-1.81
2	-4.11	-2.58
3	3.61	-0.69
4	-4.82	-1.25
5	-3.88	0.51
6	-1.92	-3.31
7	-0.65	-0.60
8	-3.20	-0.31

Table 2

The coordinates of the points in which the lines intersect the axes x_1 and x_2

line	x_1	x_2
aa	-5.95	-9.19
bb	-1.60	-1.55
cc	-7.30	-4.03
dd	-4.76	-4.59
ee	-4.65	-6.64
ff	0.40	0.21
gg	-0.59	0.50

Placed in the first line of Table 2 are the coordinates of the points in which the line aa intersects the axes of coordinates. Next we choose at random the sequence of points P_{3_i} until one of the following situations occurs: either $\Sigma(P_{3_M}) \neq \Sigma(P_1)$ and the points P_2 and P_{3_M} lie in the same half-plane with respect to the line aa , or $\Sigma(P_{3_M}) \neq \Sigma(P_2)$ and the points P_2 and P_{3_M} lie in the same half-plane. Having in this way determined $P_3 = P_{3_M}$ we run, just as before, the line bb between the point P_3 and that of the points P_1 and P_2 which belongs to the same half-plane as P_3 (see Fig. 1, Table 1 and Table 2). Then we draw the sequence of points P_{4_i} until one of the following two possibilities occurs:

1. either the point P_{4L} found itself in the figure formed by the lines drawn so far, where there already is the point P_k , $k < 4$ such that $\Sigma(P_k) \neq \Sigma(P_{4L})$,

2. or it appeared in the figure formed by the lines drawn so far where there is none of the points chosen.

This is the way we determine the point $P_4 = P_{4L}$. Further procedure depends on which of the two possibilities has taken place. In case 1, just as before, we run the line cc , dividing the points P_k and P_4 , subsequently choosing at random the sequence of points P_{5i} . In case 2 we choose at random the sequence of points P_{5i} immediately. In the situation illustrated in Fig. 1 the point P_4 found itself in the figure containing the point P_1 while at the same time $\Sigma(P_1) = 0$. Proceeding in the same way as we did while choosing at random the point P_4 we can repeat the process any number of times. However, in view of the finite dimensions of the automaton memory we have to limit ourselves to a finite number of lines (or points).

In the situation presented in Fig. 1 we have limited the number of lines to 7. In the hardware representation for a digital computer the

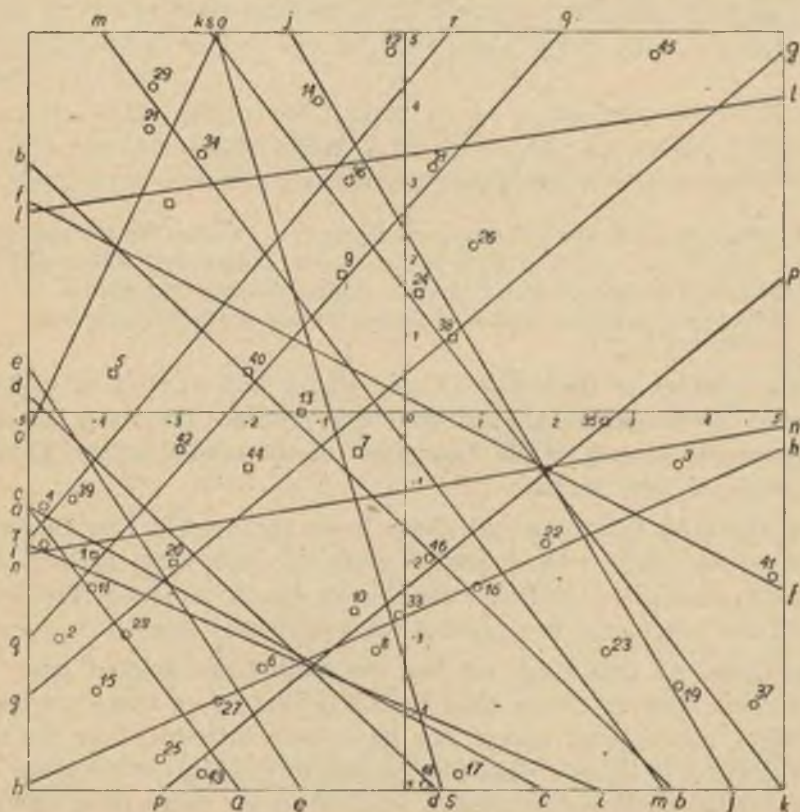


Fig. 2. Figures formed by the automaton model for $S = 19$, before the learning process.

□ — the points for which $\Sigma(P) = 0$, ○ — the points for which $\Sigma(P) = 1$

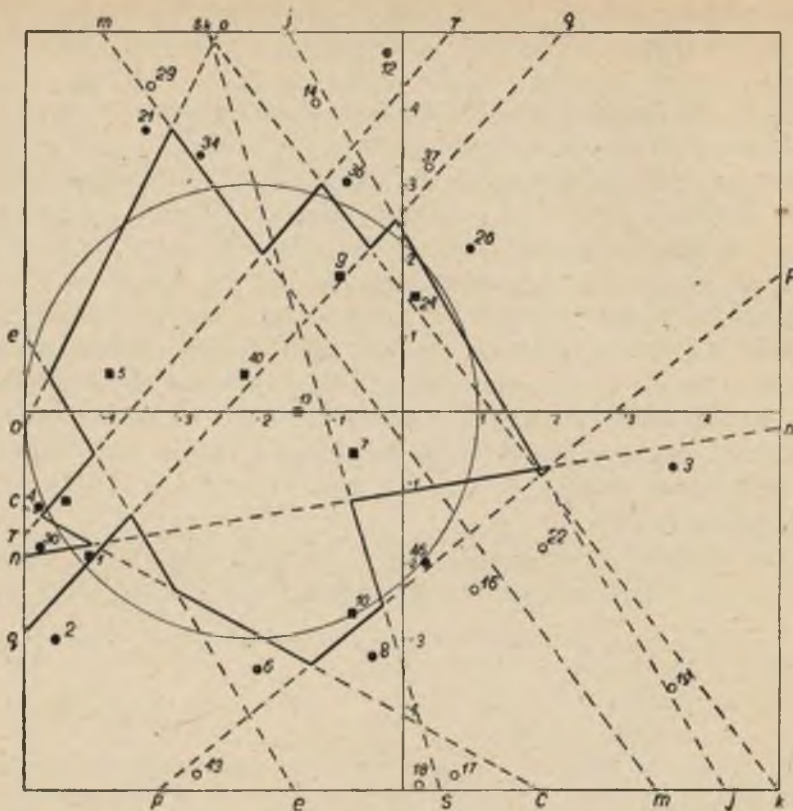


Fig. 3. Figures formed by the automaton model for $S = 19$, after the learning process
 □ — the points for which $\Sigma(P) = 0$, ○ — the points for which $\Sigma(P) = 1$,
 ■ ● — the points which were not deleted during the learning process, - - -
 — the lines and line segments deleted during the learning process

maximum number of lines was 19 (see Fig. 2 and 3). Let us call what we have so far described the introductory process. The lines having all been drawn the process of the "learning" of the model begins. This process consists of four stages:

Stage One. At this stage all these lines are deleted the deletion of which does not cause two points P_k and P_l , such that $\Sigma(P_k) \neq \Sigma(P_l)$, to appear in one figure. In Fig. 1 the line dd can be removed. The deleted lines or their fragments are marked with a dotted line.

Stage Two. At this stage all but one points are deleted from each of the figures. Let us notice that if in a given figure there are two or more points, all of them except one have been introduced as the result of the operation of stage 1 since the process of the figure formation automatically eliminated the possibility of there being more than one point in one figure. Let us also notice that for all the points P_j deleted from the given figure $\Sigma(P_j) = \Sigma(P_k)$ where k is the index of the point that

remains. Since, with the line dd removed, there is no figure in Fig. 1 which contains more than one point, no point can be deleted at this stage.

The operation at stages 3 and 4 is similar in principle to that at stages 1 and 2 except that not the whole lines but only their segments are deleted. A purely geometrical interpretation of the operation at these stages being rather difficult we shall resort to an algebraic description.

Let us first notice that each of the figures formed can be uniquely described by a certain vector with binary elements, namely by the vector $A_\mu = [\alpha_{\mu 0}, \alpha_{\mu 1}, \alpha_{\mu 2}, \dots, \alpha_{\mu S}]$ where S is the number of lines remaining after stage 1 (in the situation presented in Fig. 1, $S = 6$), $\alpha_{\mu i}$ for $i = 1, 2, \dots, S$, is equal to 0 or 1 depending on the sign of the expression: $u_i x_1 + v_i x_2 - w_i$, computed for the points of the given figure and the line i , with 0 corresponding to the nonnegative values of this expression; $\alpha_{\mu 0} = \Sigma(P_\mu)$, where P_μ is one of those randomly chosen points not deleted at stage 2 which belongs to the given figure. For instance, the figure where the point 1 in Fig. 1 belongs is described by the vector $A_1 = [0, 1, 0, 0, 0, 0, 1]$. In this way only those of the created figures can be described which contain the randomly chosen points. Thus, for example, in Fig. 1, of the total number of 14 figures remaining after the line dd has been deleted only 8 can be described. These data are gathered in Table 3.

Let the total number of figures F_μ be r , and let the total number of points remaining after stage 2 be n . Let the figures be numbered so that the first n of them contain the randomly chosen points. We shall

Table 3
Matrix A for figures appearing in Fig. 1 after the line dd is deleted

figure	line						
	α_{i0}	a	b	c	e	f	g
1	0	1	0	0	0	0	1
2	1	0	0	0	0	0	1
3	1	1	1	1	1	1	0
4	1	1	0	1	0	0	1
5	0	1	0	1	1	0	1
6	1	1	0	0	1	0	0
7	0	1	1	1	1	0	0
8	1	1	0	1	1	0	0

Table 4
Matrix B for figures appearing after the dotted line segments in Fig. 1 are deleted

figure	line						
	β_{i0}	a	b	c	e	f	g
1	0	1	0	1	0	0	1
2	0	1	0	0	1	0	1
3	0	0	0	0	0	1	1
4	0	0	0	1	1	0	1
5	0	0	0	0	1	0	1
6	0	0	0	1	0	0	1
7	0	0	1	1	0	1	1
8	0	0	1	0	0	0	1

refer to these n figures as classified, and the randomly chosen points that belong to them as classifying. Along with that we assume that if $P \in F_\mu$, then $\Sigma(P) = \Sigma(P_\mu)$ for $\mu = 1, 2, \dots, n$. The goal of stage 3 is to extend the classification to figures F_ν for $\nu = n + 1, n + 2, \dots, r$.

Stage Three. Along with the matrix $\|A_\mu\|$, the rows of which are the vectors A_μ , we shall establish the matrix $\|B_\mu\|$ with the same number of rows and columns. Initially, the binary elements of the matrix $\|B_\mu\|$ are all equal to 1 except the first column which is filled with zeroes. As stage 3 develops all the elements $\|B_\mu\|$ will be replaced by zeroes except those for which such μ' and λ , ($1 \leq \mu' \leq n$, $1 \leq \lambda \leq S$) exist that:

$$B_\mu \wedge A_\mu = B_{\mu'} \wedge A'_\mu \wedge B_\mu \text{ and } \Sigma(P_\mu) \neq \Sigma(P'_\mu) \quad (1.3)$$

where $a \wedge b$ is the Boolean product² of the binary vectors a and b and the notation $a = b$ means that the vectors a and b have the same components except may be the λ -th component. If, for given μ there are such μ' and λ that (1.3) is satisfied, element $B_{\mu\lambda}$ is left as 1.

The condition (1.3) is verified in the following order: we put $\lambda = 1$ and we verify it for all μ . Then we pass on to $\lambda = 2$, etc. The matrices $\|A_\mu\|$ and $\|B_\mu\|$ for the example presented in Fig. 1 are given in Tables 3 and 4.

As a result of the operation at this stage the unclassified figures have been joined to those classified as well as some of the boundaries (line segments) separating the figures of the same classification have been deleted. (See continuous boundaries in Fig. 1 and 3).

As a result of this process certain enlarged figures can contain more than one classifying point. The deletion of these points constitutes the fourth and the last stage of the "learning" of the model (for example, points 14, 16, 17, 18, 19, 22, 29, 37, 43 in Fig. 3). In Fig. 3, the points remaining after stage 4 are marked with black circles and squares. The deletion of all, except one, points belonging to such an enlarged figure brings economy of space in the automaton memory this being the only reason why it is used. Let us notice that a different order of carrying out the work at stage 3 may lead to different results, i.e., the unclassified figures may get joined to other classified figures than it has been the case with this order. The actual order of this procedure, and for the procedure realizing the stages 1 and 2 is given in [2].

The "learning" of the model over, it is possible to classify each point $P_j \in K$. This will consist in determining the function $\Sigma'(P_j)$ in the following way:

Having the coordinates of the point $P_j = (x_{1j}, x_{2j})$ we establish the vector $A_j = [a_{j0}, a_{j1}, a_{j2}, \dots, a_{js}]$, where a_{j0} is the unknown, and we determine $a_{j1}, a_{j2}, \dots, a_{js}$ in a similar way as the elements of the matrix $\|A_\mu\|$. Then we find out for the consecutive $\mu = 1, 2, \dots, n$ whether the following relation holds:

$$B_\mu \wedge A_j = B_\mu \wedge A_\mu. \quad (1.4)$$

² We call the Boolean product of the vectors $a = [a_1, a_2, \dots, a_n]$ and $b = [b_1, b_2, \dots, b_n]$ the vector $a \wedge b = c = [c_1, c_2, \dots, c_n]$, where $c_i = a_i \times b_i$.

It follows from the process of "learning" described above that there exists one and only one μ such that the above equality holds for it and then we assume:

$$a_{j0} = \Sigma'(P_j) = \Sigma(P_\mu) = a_{\mu 0}.$$

We interpret the obtained result as an assertion that the solution of the system of equations (1.1) with the initial data $(x_1^0, x_2^0) = P_j$ will remain within the area K , during the time T , if $a_{j0} = 0$ and will leave this area otherwise. For the situation presented in Fig. 1 let us consider the example $P_j = (2.5, 3.5)$ (the point marked with a cross). The vector A_j has the coordinates $[a_{j0}, 1, 1, 1, 1, 1, 1]$. Verifying the condition (1.4) we notice that it is satisfied for $\mu = 5$, i.e., $a_{j0} = a_{\mu 0} = 0$. On a digital computer $\Sigma'(P)$ is found much faster than $\Sigma(P)$.

Of course, the quality of the classification (the accuracy of the approximation of the set X by the union of all the figures F_σ such that $\Sigma(P_\sigma) = 0$) improves with the number of the lines employed (cf. Fig. 1 with Fig. 3). This accuracy can be determined in the following way:

Let us perform a test which consists in choosing at random the coordinates of the points $P_j = (x_{1j}, x_{2j})$, $j = 1, 2, \dots, N$, $P_j \in K'$. For each of these points we shall determine the function $\Sigma(P_j)$ by means of the numerical integration of equations (1.1) and the function $\Sigma'(P_j)$ by means of the method described above. Let us define by I the number of points P_j for which $\Sigma(P_j) \neq \Sigma'(P_j)$. For a sufficiently large N it will be possible to treat the ratio I/N as the ratio of the Lebesgue measures of the set $D(\bigcup_{\sigma} F_\sigma, X)$, where $D(A, B)$ is the difference, in the sense of Frechet and Nikodym, of the sets A and B , i.e., $D(A, B) = (A \cup B) \dot{-} (A \cap B)$ (the symbol $\dot{-}$ denotes the subtraction of sets), and $\bigcup_{\sigma} F_\sigma$ is the union of all the figures for which $\Sigma(P_\sigma) = 0$, and of the set K' : $I/N = \mu(D(\bigcup_{\sigma} F_\sigma, X)) / \mu(K')$.

Since, as a result of the process of "learning", the number of lines and points is usually reduced, we can add all or part of the points for which $\Sigma(P_j) \neq \Sigma'(P_j)$ to the respective tables and draw additional lines, i.e., for each of these points in succession we repeat the operations described in the first part of this chapter. Having allocated all the memory space intended for table storage (or having exhausted the list of points classified in different ways), we renew the "learning" of the model. We shall call the processes of "learning", the tests and the addition of the points (and the corresponding lines) used in the tests to the tables of the model the process of generalization. It is to be emphasized that the process of learning we pass on to right after the memory space has been exhausted, no longer belongs to the first process of generalization but is the first phase of the next process of generalization. We can repeat the process of generalization until we have achieved the required accuracy or until the

situation occurs in which the number of lines and points does not get reduced by the process of "learning". Let us notice that we must not expect the accuracy to be too great since, for example, using not more than 19 lines we can obtain the best approximation of the area X , which is a circle, if $\bigcup_{\sigma} F_{\sigma}$ is a regular nonadecagon circumscribed about this circle. For such approximation the relation I/N (for a sufficiently great N) will be equal to 0.0024. Aside from the evaluation of accuracy which is given by I/N , interesting conclusions concerning the quality of the approximation can be drawn from a visual comparison of $\bigcup_{\sigma} F_{\sigma}$ and X , assuming, of course, that the set X is known (as is the case here). The reconstruction of the geometrical form of $\bigcup_{\sigma} F_{\sigma}$ on the basis of the data from the sufficiently large tables similar to 1, 2, 3 and 4 is rather laborious (cf. Fig. 2 and 3 obtained in this way). In connection with this a simple method has been employed allowing for the geometrical construction of the set $\bigcup_{\sigma} F_{\sigma}$ by the computer itself. The method makes use of the standard teleprinter equipment.

Let us consider the area in the form of a square with side 10 and the center in the origin of the coordinate system, and a sequence of points $P_{ij} = (x_{1i}, x_{2j})$ determined by:

$$x_{1i} = -5 + i \frac{10}{l_{x_1}}, \quad x_{2j} = 5 - j \frac{10}{l_{x_2}}, \quad \begin{matrix} i = 0, 1, \dots, l_{x_1} \\ j = 0, 1, \dots, l_{x_2} \end{matrix}$$

where the numbers l_{x_1} and l_{x_2} are determined as follows: l_{x_1} is the number of characters in a conventional teleprinter line augmented by one ($l_{x_1} = 60$), and l_{x_2} has been selected so that $l_{x_1} \times sh = l_{x_2} \times sw$, where sh is the distance between the centers of the consecutive teleprinter symbols in the line, and sw is the distance between the consecutive lines measured between the symbol centers. We determine the function $\Sigma'(P_{ij})$ for each point P_{ij} and in the appropriate space of the teleprinter sheet we print the $+$ sign, if $\Sigma'(P_{ij}) = 0$, or the "symbol of space" (blank) when $\Sigma'(P_{ij}) = 1$. The initial square K' is the inside of the figure enclosed in a frame of small squares. Fig. 4-8 present the very kind of sets $(\bigcup_{\sigma} F_{\sigma})_i$ drawn

by the computer at the end of the consecutive processes of "learning", the configurations brought outside the computer being only those for which $I_j/N_j < I_{j-1}/N_{j-1}$ held. The respective values of $1 - I_j/N_j$ are indicated under each figure. In order to facilitate comparisons the coordinate axes and the real area X have been plotted on the computer-produced figures. Since in all the examples presented in Fig. 4-8 N_j was relatively small, the quotients I_j/N_j are not too plausible evaluations of accuracy. Thus, for instance, a considerably more plausible estimate for Fig. 8, obtained by counting the crosses going outside the

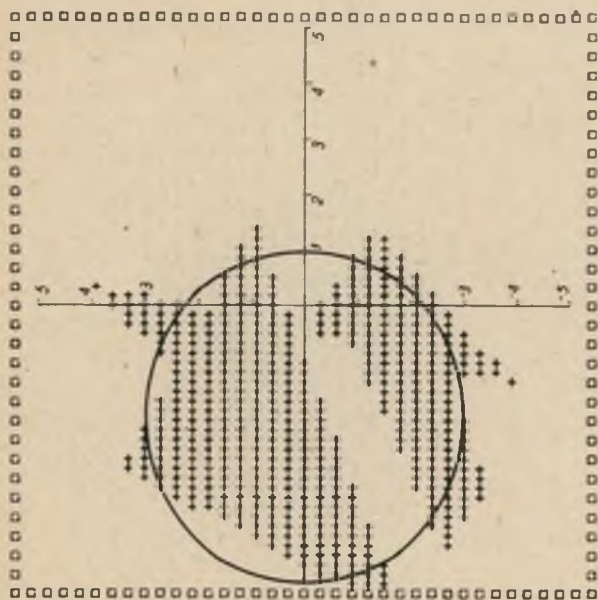


Fig. 4. Set $(\bigcup_{\theta} E_{\theta})_1$, $1 - I/N = 1 - 59/64$

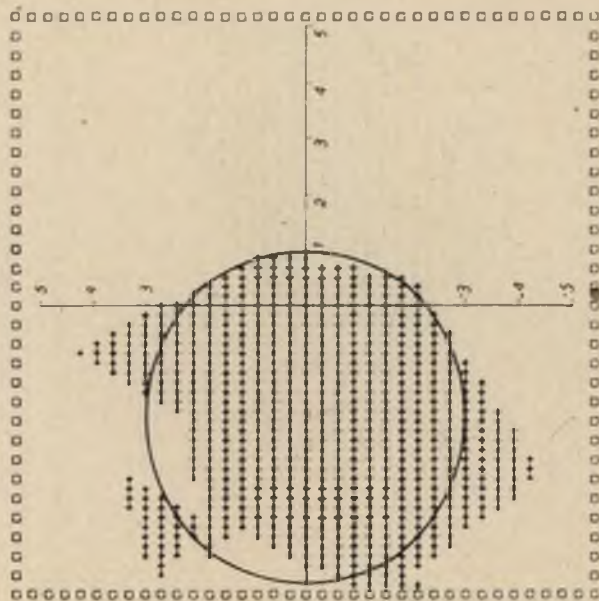


Fig. 5. Set $(\bigcup_{\sigma} F_{\sigma})_2$, $1 - I/N = 1 - 61/64$

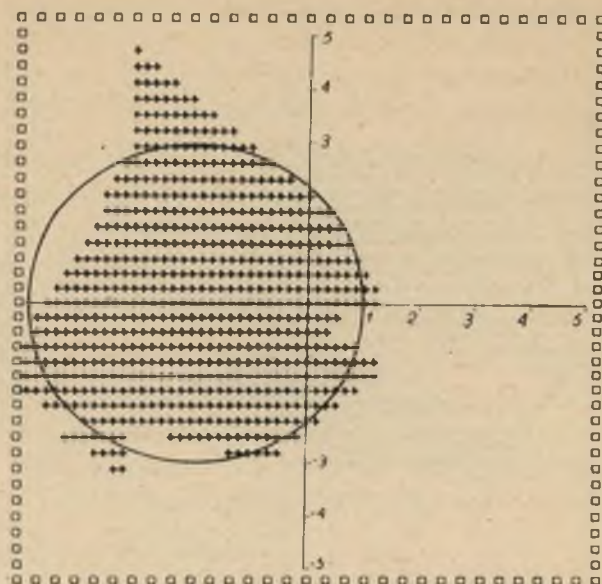


Fig. 6. Set $(\bigcup_{\sigma} F_{\sigma})_3$, $1 - I/N = 1 - 62/64$

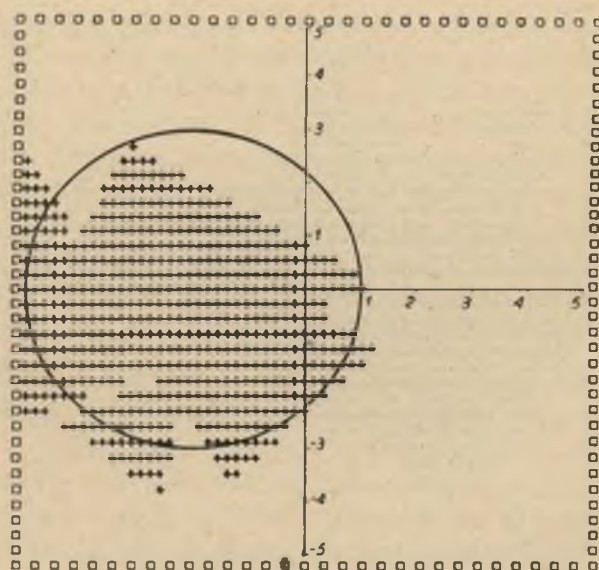


Fig. 7. Set $(\bigcup_{\sigma} F_{\sigma})_4$, $1 - I/N = 1 - 63/64$

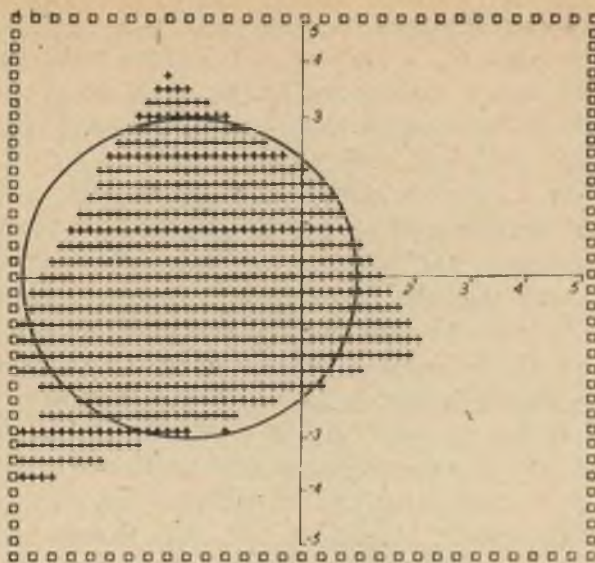


Fig. 8. Set $(\bigcup_{\sigma} F_{\sigma})_5$, $1 - I/N = 1 - 64/64$

marked circle and the blanks inside the circle, was $1 - I/N = 1 - 168/2800 = 0.94$.

2. Some Remarks on the Statistical Interpretation of the Notion of Practical Stability

Let us consider a vector equation with perturbations:

$$x' = f(t, x) + \pi(t, x) \quad (2.1)$$

where x is a vector in an n -dimensional Euclidean space E^n , t is a scalar variable while f and π are vector functions with values in E^n .

We shall assume that:

1. the function $\pi \in \Pi$, where Π is the family of all the possible perturbing functions satisfying some condition of "smallness",
2. the function f and all the functions from π are determined in the closed cylinder $W = \mathcal{X} \times I_T$, where $I_T = [0, T]$, and in this cylinder they satisfy Tonelli's condition ([4] p. 4),
3. $f(0, t) = 0$ for all $t \in [0, T]$.

Let us further consider a finite time interval $[0, \tau]$, where $0 < \tau \leq T$, and the set $K \subset \mathcal{X}$, $0 \in K$. Let us assume that on the set \mathcal{X} the function $p(x)$ is determined which is equal, for each $x^0 \in \mathcal{X}$, to the probability of the event consisting in that the solution of the equation (2.1) with the randomly chosen function $\pi \in \Pi$, satisfying the initial condition $x(0) = x^0$, will satisfy the condition:

$$x(t) \in K \text{ for } t \in [0, \tau]. \quad (2.2)$$

Let X_ε be the set of points for which $p(x) > 1 - \varepsilon$. If ε is equal to 0, we shall assume that $X_0 = \{x: p(x) = 1\}$. Along with the sets X_ε we shall consider the set X determined as the set of all the points x^0 , such that the solution of the equation (2.1) with the initial condition $x(0) = x^0$, for any function $\pi \in \Pi$, will satisfy the condition: $x(t) \in K$ for $t \in [0, T]$. Between the sets X_0 and X the relationship: $X \subset X_0$ holds. Indeed, it follows from the definition of the set X that for each $x^0 \in X$ the solution (2.1) with the function $\pi \in \Pi$ and the condition $x(0) = x^0$ will satisfy the condition (2.2), and thus the probability of the event consisting in that the solution (2.2) with the randomly chosen function $\pi \in \Pi$ and the condition $x(0) = x^0$ will be equal to 1, i.e., $p(x^0) = 1$, thus $x^0 \in X_0$. Let us notice that the inverse inclusion ($X_0 \subset X$) does not have to be true in general, i.e., it is not necessary for $X = X_0$ to be true. In fact, if, for example, the family Π contains an infinite multitude of functions π and for the given x^0 the condition (2.2) is satisfied for all except the finite number of functions $\pi \in \Pi$, then $p(x^0) = 1$ even though there exist solutions which do not satisfy the condition (2.2), and thus $x^0 \in X_0 \setminus X$.

When controlling dynamic processes it is important to be able to answer the question whether the created initial conditions x^0 are a guarantee, with the probability not less than $1 - \varepsilon$, $\varepsilon > 0$, for the process to be carried out so that the trajectory, which represents the process, does not leave the area K of the phase space during the time $[0, \tau]$, i.e., in other words, whether $x^0 \in X_\varepsilon$ holds. The next chapter of our paper will be concerned with applying the model described in the preceding chapter to the solution of this problem.

To conclude this chapter let us examine an instructive example of the equation (2.1). Let the following system of equations be given:

$$\frac{dx_1}{dt} = x_1 + x_2 + \pi_1(x_1, x_2, t), \quad \frac{dx_2}{dt} = x_1 - x_2 + \pi_2(x_1, x_2, t) \quad (2.3)$$

where $|\pi_i(x_1, x_2, t)| \leq \min(|x_1 + (-1)^{i-1}x_2|, \delta)$, $\delta > 0$. Let the area K be the square: $K = \{(x_1, x_2): -1 \leq x_1 \leq 1, -1 \leq x_2 \leq 1\}$ and $\tau = 1$. Let us examine the system of equations:

$$\frac{dx_1}{dt} = x_1 + x_2, \quad \frac{dx_2}{dt} = x_1 - x_2, \quad (2.4)$$

following from (2.3) when $\pi_1 = \pi_2 = 0$. The general set of solutions of this system is:

$$\begin{aligned} \tilde{x}_1(t) &= \frac{1}{2\sqrt{2}} [ae^{\sqrt{2}t} - be^{-\sqrt{2}t}], & \tilde{x}_2(t) &= \frac{1}{2\sqrt{2}} [ce^{\sqrt{2}t} - de^{-\sqrt{2}t}], \\ a &= x_1^0 + x_2^0 + \sqrt{2}x_1^0, & c &= x_1^0 - x_2^0 + \sqrt{2}x_2^0, \\ b &= a - 2\sqrt{2}x_1^0, & d &= c - 2\sqrt{2}x_2^0. \end{aligned} \quad (2.5)$$

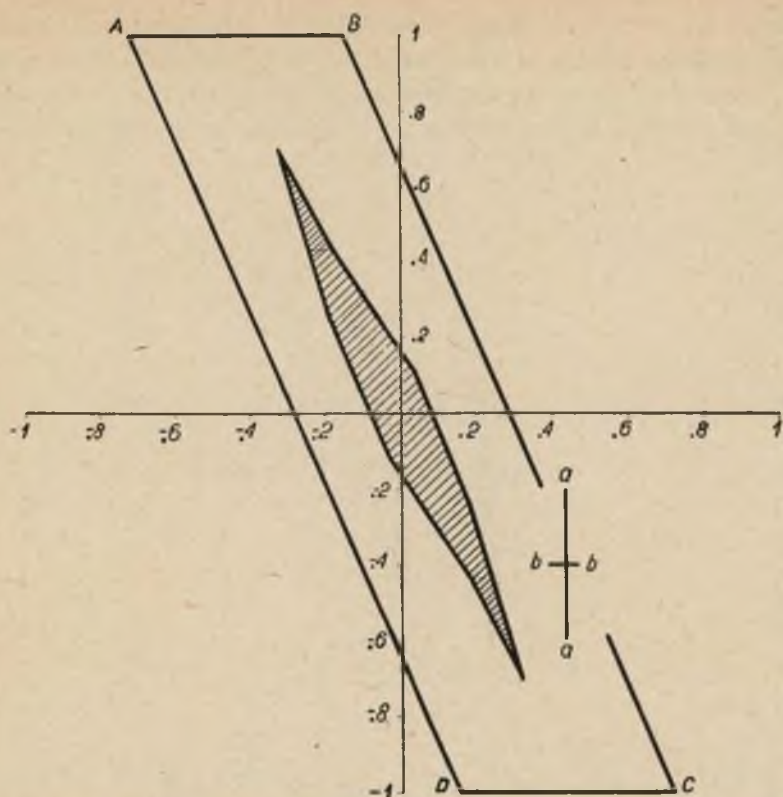


Fig. 9. Set X for the equations (2.3) — shaded figure and for the equations (2.4) — $ABCD$

In Fig. 9 the parallelogram $ABCD$ is a set of initial conditions such that the solutions (2.5) will not leave the area K during the time $[0, 1]$. It can be demonstrated that:

$$x_1(t) - \bar{x}_1(t) = \frac{1}{2} \int_0^{\sqrt{2}t} [(\pi_1(x_1, x_2, u) + \pi_2(x_1, x_2, u)) \operatorname{sh} \xi + \sqrt{2} \pi_1(x_1, x_2, u) \operatorname{ch} \xi] d\xi$$

$$x_2(t) - \bar{x}_2(t) = \frac{1}{2} \int_0^{\sqrt{2}t} [\pi_1(x_1, x_2, u) \operatorname{sh} \xi + \pi_2(x_1, x_2, u) (\sqrt{2} \operatorname{ch} \xi - \operatorname{sh} \xi)] d\xi,$$

where $u = t - \frac{\xi}{\sqrt{2}}$.

It is not difficult to see that the greatest positive (negative) deviations appear with the extremal "steering" of the perturbations π , i.e., when it holds:

for the positive ones:

$$\pi_1(x_1, x_2, u) = \min(\delta, |x_1 + x_2|),$$

$$\pi_2(x_1, x_2, u) = \min(\delta, |x_1 - x_2|),$$

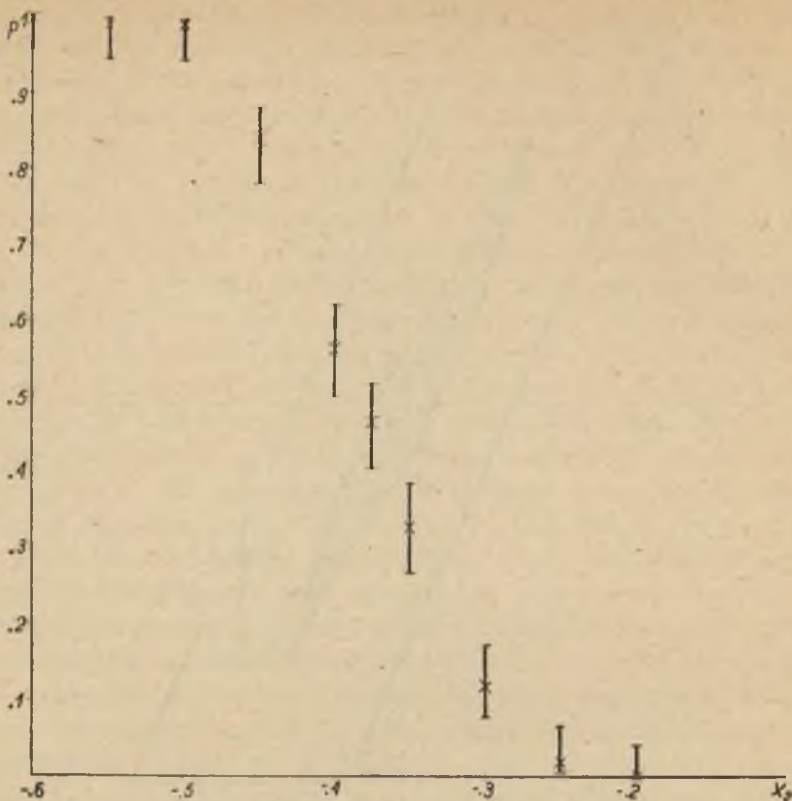


Fig. 10. Values of the probability of $p(x)$ along the section aa

for the negative ones:

$$\pi_1(x_1, x_2, u) = \max(-\delta, -|x_1 + x_2|),$$

$$\pi_2(x_1, x_2, u) = \max(-\delta, -|x_1 - x_2|).$$

Of course, the set X is included in the parallelogram $ABCD$ and if the perturbed trajectory leaves the square K , it intersects its sides perpendicular to the axis x_1 . The region X can be determined as the locus of all the points with no such extremal trajectory originating from them which intersects the sides of the square K during the time $[0, 1]$. The set X has been determined experimentally on the GIER computer owned by the University of Warsaw.

This method of determination is roughly similar to the technique used for making figures which was described at the end of the preceding chapter except that a very fine grid was employed there and both extremal trajectories were drawn from each node of the grid. The point was assigned to the area X if none of the trajectories had left the square.

The area X is presented in the shaded figure in Fig. 9. To examine the behavior of the function $p(x)$ its values were found for a number of points belonging to two perpendicular segments which intersected at a point lying outside X (see the segments aa and bb in Fig. 9). The results of the

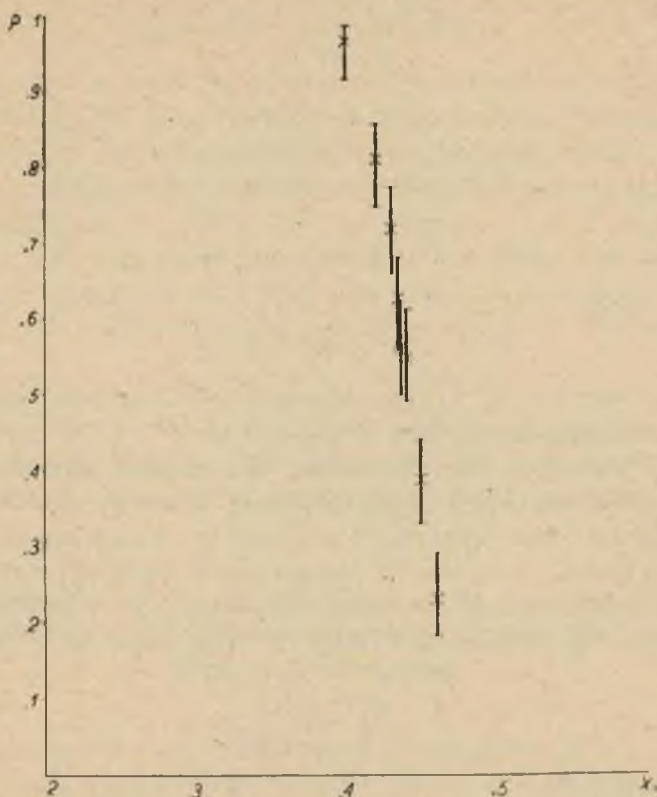


Fig. 11. Values of the probability of $p(x)$ along the section bb

examination are presented in Fig. 10 and 11. A correct interpretation of these figures requires some familiarity with the method used for obtaining them. Let us consider the point (x_1^0, x_2^0) and perform the numerical integration of equations (2.3) by employing the modified method of Runge-Kutta-Gill [2]³. These n trajectories can be regarded, for a suffi-

³ The modification of the method of Runge-Kutta-Gill consisted in that whenever the values of the right-hand sides of the equations were computed, the formula $f_i = x_1 + (-1)^{1-i} x_2 + r_i$ was used where r_i is a random number from the interval

$$[-\min(|x_1 + (-1)^{1-i} x_2|, 0.5), \min(|x_1 + (-1)^{1-i} x_2|, 0.5)].$$

The experiments being carried out with the aid of programs written in the ALGOL language, the generator mentioned in Note 1 could not be applied without a complicated adaptation. For this reason another generator of pseudo-random numbers was used, based on the procedure communicated to us by Chr. Gram.

ciently large n , as a statistical sample drawn from the family of all the possible trajectories of the equations (2.3) with the initial condition $x^0 = x(0)$, and, if out of these n trajectories m trajectories will leave the square K at the time $[0, 1]$, then it can be assumed that:

$$p(x_1^0, x_2^0) = 1 - m/n. \quad (2.7)$$

The number of the trajectories n was selected so as to keep the plausibility of the approximation (2.7), according to the law of Bernoulli [5], independent of the obtained value p . Thus, after we have determined two non-negative numbers ε and η we select n so that:

$$P\left(\left|1 - \frac{m}{n} - p(x^0)\right| < \varepsilon\right) \geq 1 - \eta,$$

which holds when:

$$n > \frac{p(x^0)[1 - p(x^0)]}{\varepsilon^2 \eta}$$

In the experiments carried out $\varepsilon = \eta = 0.1$.

It can be seen from the above that the greatest number of trajectories to be examined is at $p(x^0) = 0.5$. Since, however, prior to the experiment we do not know what $p(x^0)$ amounts to, we are equally ignorant of what n to assume to make the expression $1 - m/n$ approximate $p(x^0)$ with the required accuracy. To begin with we assume that $p(x^0) = 1 - \varepsilon$, which gives us the minimum number of trajectories to be examined⁴:

$$n_1 = E\left[\frac{(1 - \varepsilon)}{\varepsilon \eta}\right] + 1$$

(in our case $n_1 = 91$).

From this examination we shall obtain a certain value m_1/n_1 and, consequently, the number of further trajectories to be examined:

$$n_2 = \begin{cases} E\left[\frac{\left(\frac{m_1}{n_1} - \varepsilon\right)\left[1 - \left(\frac{m_1}{n_1} - \varepsilon\right)\right]}{\varepsilon^2 \eta}\right] + 1 - n_1, & \text{when } \frac{m_1}{n_1} \geq 0.5 + \varepsilon, \\ E\left[\frac{0.25}{\varepsilon^2 \eta}\right] + 1 - n_1, & \text{,, } 0.5 - \varepsilon \leq \frac{m_1}{n_1} < 0.5 + \varepsilon \\ E\left[\frac{\left(\frac{m_1}{n_1} + \varepsilon\right)\left[1 - \left(\frac{m_1}{n_1} + \varepsilon\right)\right]}{\varepsilon^2 \eta}\right] + 1 - n_1, & \text{,, } \frac{m_1}{n_1} < 0.5 - \varepsilon. \end{cases}$$

After carrying out the second series of tests we obtain a more plausible

⁴ $E(a)$ denotes that only the integral part of the number a is taken into account.

approximation $p(x^0) = 1 - \frac{m_1 + m_2}{n_1 + n_2}$. This process will be repeated until $n_2 = 0$ occurs. Then we have, with the prescribed accuracy:

$$p(x^0) = 1 - \frac{\sum_i m_i}{\sum_i n_i} = 1 - m/n.$$

Plotted in the graphs (Fig. 10 and 11) are the points corresponding to the expressions $1 - m/n$, together with their confidence intervals obtained by means of Gauss-Laplace theorem for confidence level 0.95.

It is worth while to notice the fact, which is made clear by both the graphs, that for points lying rather far from the area X the function $p(x^0)$ assumes values which are close to 1. Roughly speaking, the areas X_ε are considerably "larger" than the area X even for very small $\varepsilon > 0$.

The results presented in the graphs, as well as the results of the experiments described in the next chapter, seem to confirm the intuitively obvious conclusion that $X_{0.5}$ for equations with perturbations roughly coincides with the area X for equations without perturbations.

3. The Application of the Digital Model of the Learning Automaton to the Examination of Practical Stability Taking into Account Random Perturbations

In this chapter we shall describe the application of the automaton model to the solution of the following problem: We are given the equation (2.1), the set K , the finite time interval $[0, \tau]$ and the perturbation family Π (notations of Ch. 2). We are also given the sequence of the initial data $x^{01}, x^{02}, \dots, x^{0i} \dots$ belonging to K . We are to determine for each x^{0i} whether the solution of the equation (2.1) with the initial condition $x(0) = x^{0i}$ will remain in the area K within the time τ . Since we do not know which of the functions of the family Π will enter the equation (2.1) the answer to the question posed in this manner cannot always be unique.

This ambiguity can be removed if we find a non-negative number ε such that in a sufficiently long sequence of n answers there will be no more than εn incorrect answers, our judgement as to the correctness or incorrectness of the answers being based on the observation of the physical dynamic system the mathematical description of which is the equation (2.1). Of course, the observation of the physical system can be replaced by the observation of the behaviour of the digital model of this system, i.e., for example, by the examination of the trajectories of

the equation (2.1) for which the functions π have been chosen from the family Π according to the same law which governs the distribution of perturbations taking place in the physical object. We shall describe the operation of the automaton model in solving the problem described above by employing the following example:

Let us examine the system of equations:

$$\begin{aligned}\frac{dx_1}{dt} &= x_2 + \pi_1(t), \\ \frac{dx_2}{dt} &= x_1 + \lambda(x_1^2 - 1)x_2 + \pi_2(t), \quad \lambda > 0.\end{aligned}\tag{3.1}$$

For $\pi_1 = \pi_2 = 0$ the system represents the Van der Pol equation. The value of λ in this example was equal to 3. Let us here assume that the area K is bounded by only two horizontal lines⁵:

$$x_1 = 4, x_1 = -4.$$

The system of equations (3.1) has, for $\pi_1 = \pi_2 = 0$ and for $\lambda = 3$ the periodic solution with the period $T = 8.8613$ intersecting the axis x_1 at the point $x_1 = 2.0235$ [6]. This solution is presented in Fig. 12-16 (the figure drawn with a continuous line). Owing to the special character of Van der Pol's equation, the time τ has been chosen so that $\tau > 0.5 T$, more specifically, $\tau = 5$. We shall define the family of perturbations Π as the set of all functions $\pi(t)$ assuming, in the finite number of points $t^i \in [0, \tau]$ the values which are random numbers from the interval $[-0.02, 0.02]$ and choose the numerical values of perturbations correspondingly. Also, in view of the equation it can be assumed that the set X is contained in the square K' bounded by the lines:

$$x_1 = -4, x_1 = 4, x_2 = -6, x_2 = 6.$$

The operation of the automaton model in solving this kind of problem breaks up into a number of levels $L_i, i = 0, 1, \dots$. The level L_0 is identical with the process described in Ch. 1. Each of the processes $L_i, i \neq 0$, consists of a number of processes of generalization $G_{i\mu}$ (the notations of Ch. 2). It will be recalled that every process of generalization provides an estimate of the accuracy of the approximation achieved by this process, $1 - m_{i\mu}$. This estimate is now determined in a slightly different fashion than in Ch. 1, because of some difference in the classification

⁵ The limitation of the area K in but one dimension follows from the physical interpretation of the system (3.1) without perturbations which is equivalent to the second order equation

$$\frac{d^2x}{dt^2} - (x^2 - 1)\frac{dx}{dt} + x = 0.$$

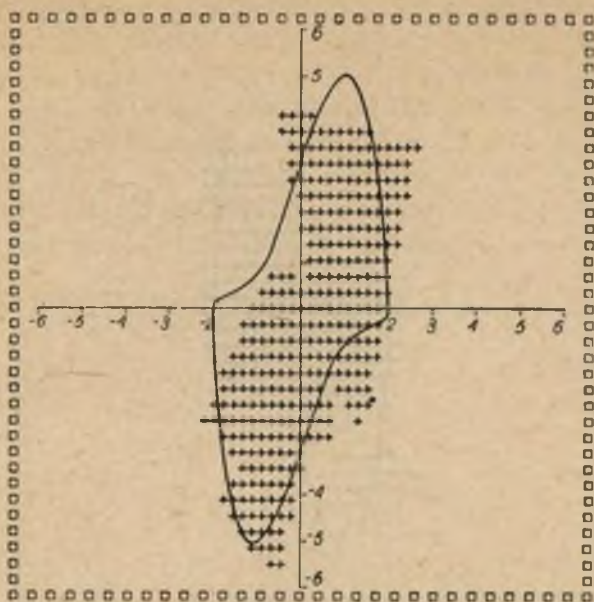


Fig. 12. $L_1, G_{11}, m_1 = 10/128, b_1 = 4/128$. Set U — figure marked with crosses, periodic solution of equations (3.1) without perturbations — continuous line

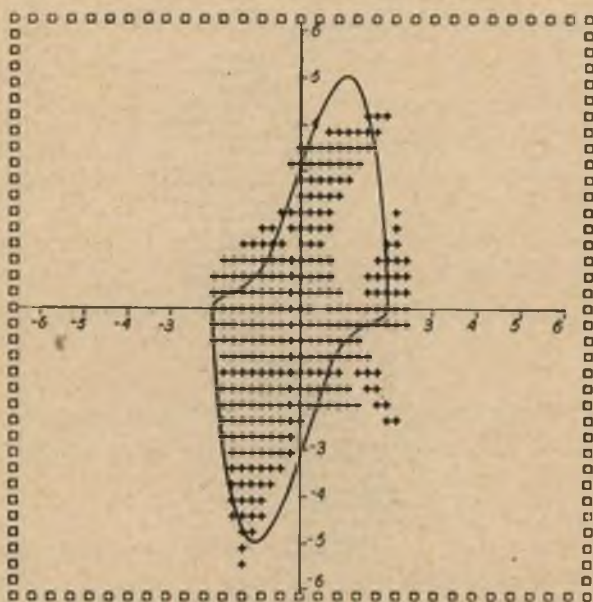


Fig. 13. $L_1, G_{11}, m_{11} = 19/128, b_{11} = 8/128$. Set U — figure marked with crosses, periodic solution of equations (3.1) without perturbations — continuous line

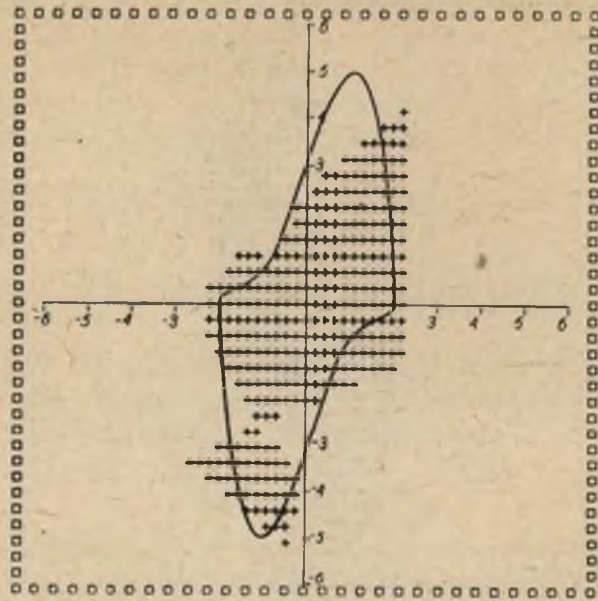


Fig. 14. $L_2, G_{25}, m_{25} = 9/128, b_{25} = 4/128$. Set U — figure marked with crosses, periodic solution of equations (3.1) without perturbations — continuous line

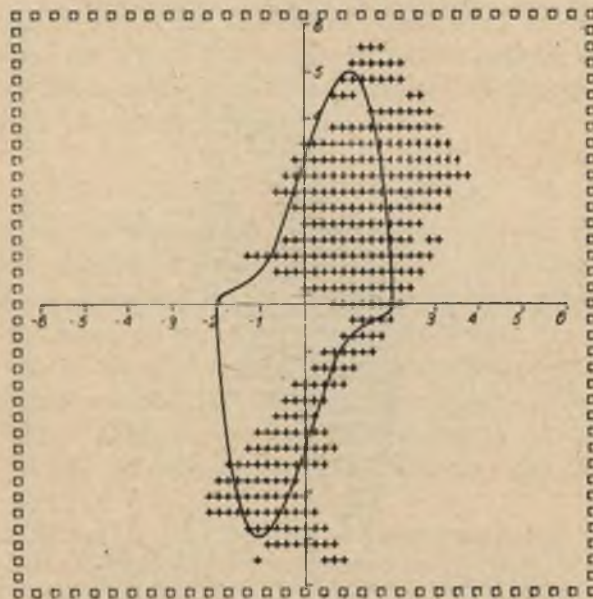


Fig. 15. $L_3, G_{36}, m_{36} = 20/128, b_{36} = 10/128$. Set U — figure marked with crosses, periodic solution of equations (3.1) without perturbations — continuous line

of points, viz., instead of the function $\Sigma(x_1, x_2)$ being uniformly determined for all the processes of generalization we shall examine the sequence of functions $\Sigma_i(x_1, x_2)$ determined for the given level L_i as follows: from the point (x_1^0, x_2^0) , chosen at random, we run (using the method of numerical integration) $i+1$ trajectories which correspond to π_1 and π_2 chosen at random. If none of these trajectories leave the area K within the time $[0, \tau]$, then $\Sigma_i(x_1^0, x_2^0) = 0$, otherwise $\Sigma_i(x_1^0, x_2^0) = 1$. The determination of the function $\Sigma'(x_1^0, x_2^0)$ will remain unchanged and it is only for the sake of symmetry that we shall introduce the notation $\Sigma'_i(x_1, x_2)$. Let us choose

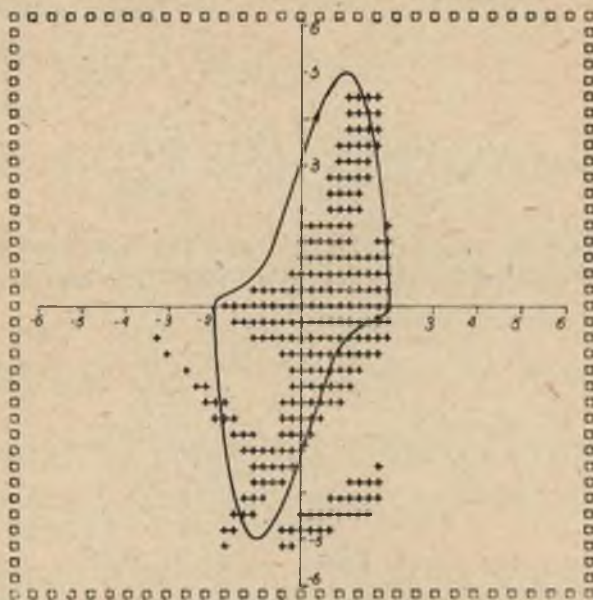


Fig. 16. $L_3, G_{38}, m_{38} = m_3 = 7/128, b_{38} = b_3 = 3/128$. Set U — figure marked with crosses, periodic solution of equations (3.1) without perturbations — continuous line

at random N points P_j from the area K . For each of them we determine the value $\Sigma'_i(P_j)$ and compute $\Sigma_i(P_j)$. Let M be the number of points for which the following holds:

$$\Sigma'_i(P_j) \neq \Sigma_i(P_j),$$

and let B be the number of points P_j for which the above mentioned condition is satisfied, and, in addition to this:

$$\Sigma'_i(P_j) = 0.$$

Let us denote: $m_i = M/N, b_i = B/N$.

Let us examine the sets X_0 and X_1 (for notations see Ch. 2).

Let $U = \bigcup_{\sigma} F_{\sigma}$. Let us denote:

$$\bar{X} = X_1 \div X_0, X^* = K' \div X_1.$$

Let us assume that the sets K' , X^* , \bar{X} , and U are measurable in the sense of Lebesgue. In our further considerations we shall employ the so-called normalized Lebesgue measure determined by $\text{mes}(A) = \mu(A)/\mu(K')$, for all $A \subset K'$, where $\mu(C)$ denotes the Lebesgue measure of the set C . We shall denote the integration with respect to this measure by $\int_A f dx$, where f is an arbitrary integrable function.

For a sufficiently large N we have:

$$m_{i_r} = \int_{K'} \varrho(x) dx = \int_{U \cap X_0} \varrho(x) dx + \int_{X_0 \div U} \varrho(x) dx + \int_{U \cap \bar{X}} \varrho(x) dx + \int_{\bar{X} \div U} \varrho(x) dx + \int_{U \cap X^*} \varrho(x) dx + \int_{X^* \div U} \varrho(x) dx, \quad (3.2)$$

where

$$\varrho(x) = \begin{cases} [p(x)]^{i+1} & \text{for } x \notin U, \\ 1 - [p(x)]^{i+1} & \text{for } x \in U. \end{cases}$$

It is not difficult to see that the first and the last term in the formula (3.2) are equal to 0, while the second and the fifth one are equal to, respectively, $\text{mes}(X_0 \div U)$ and $\text{mes}(U \cap X^*)$.

$$\begin{aligned} m_{i_r} &= \text{mes}(X_0 \div U) + \text{mes}(U \cap X^*) + \int_{U \cap \bar{X}} (1 - [p(x)]^{i+1}) dx + \\ &+ \int_{\bar{X} \div U} [p(x)]^{i+1} dx = \text{mes}(X_0 \div U) + \text{mes}(U \cap X^*) + \text{mes}(U \cap \bar{X}) + \\ &+ \int_{\bar{X} \div U} [p(x)]^{i+1} dx - \int_{U \cap \bar{X}} [p(x)]^{i+1} dx \end{aligned} \quad (3.3)$$

Since all the sets over which we integrate in the formula (3.2) are disjoint and $U \cap \bar{X} \cup U \cap X^* = U \div X_0$, then

$$m_{i_r} = \text{mes}[D(U, X_0)] + \int_{\bar{X} \div U} [p(x)]^{i+1} dx - \int_{U \cap \bar{X}} [p(x)]^{i+1} dx. \quad (3.4)$$

In a similar way, we can obtain:

$$b_{i_r} = \text{mes}(U \div X_0) - \int_{U \cap \bar{X}} [p(x)]^{i+1} dx. \quad (3.5)$$

Depending on the application, either $\text{mes}[D(U, X_0)]$ or $\text{mes}(U \div X_0)$ can be adopted as the measure of accuracy.

From the formulas (3.4) and (3.5) we easily obtain:

$$\begin{aligned} |\text{mes}[D(U, X_0)] - m_{i_r}| &< \int_{\bar{X}} [p(x)]^{i+1} dx, \\ |\text{mes}(U \div X_0) - b_{i_r}| &< \int_{\bar{X}} [p(x)]^{i+1} dx. \end{aligned} \quad (3.6)$$

It is worth while noting that the upper bounds of error in the estimates of the respective numbers m_{i_v} and b_{i_v} are independent of the shape of U , and that, as we pass on to the higher levels, they decrease, since for $x \in \bar{X}$ $p(x) < 1$. Let us note as a curiosity that at the given L_i the numbers m_i have the lower bound and $\inf m_{i_v} = 0$ if and only if $\text{mes}(\bar{X}) = 0$. In fact, it follows from the formula (3.3) that:

$$m_{i_v} \geq \int_{U \cap \bar{X}} (1 - [p(x)]^{i+1}) dx + \int_{\bar{X} - U} [p(x)]^{i+1} dx \quad (3.7)$$

the equality holding when

$$\text{mes}(X_0 - U) = \text{mes}(U \cap X^*) = 0.$$

On the other hand

$$\int_{U \cap \bar{X}} (1 - [p(x)]^{i+1}) dx + \int_{\bar{X} - U} [p(x)]^{i+1} dx \geq \int_{A_1} (1 - [p(x)]^{i+1}) dx + \int_{A_2} [p(x)]^{i+1} dx \quad (3.8)$$

where A_1 and A_2 are derived by dividing the set \bar{X} so that

$$A_1 = \{x: 0.5 < p(x)^{i+1} < 1\}, A_2 = \{x: 0 < p(x)^{i+1} \leq 0.5\}, A_1 \cup A_2 = \bar{X}.$$

In this kind of division:

$$U = X_\varepsilon, \text{ where } \varepsilon = 1 - 2^{-\frac{1}{i+1}} \quad (3.9)$$

$$\int_{A_1} (1 - [p(x)]^{i+1}) dx + \int_{A_2} [p(x)]^{i+1} dx > \frac{1}{2} \text{mes}(A_1) + \frac{1}{2} \text{mes}(A_2) = \frac{1}{2} \text{mes}(\bar{X}).$$

The processes of generalization at the given level L_i are repeated until we obtain $m_{is} < m_{i-1}$. Having obtained such s we put $m_i = m_{is}$. By definition for $i = 0$ we assume $m_0 = 1$. Having finished our work at the i -th level we go over to the level L_{i+1} . The transition to this level consists in that we verify the classification of the points P_σ , that is, we run an additional, "random" trajectory for those of the points P_σ for which $\alpha_{\sigma 0} = 0$, and we change $\alpha_{\sigma 0}$ to 1 if the trajectory leaves the area K within the time τ . Having verified the work, we can begin at the level L_{i+1} . If we continued the process for $i \rightarrow \infty$, then $\varepsilon \rightarrow 0$ and the integrals in the formulas (3.6) tend to 0 because for points belonging to \bar{X} , $p(x) < 1$ holds. Thus:

$$m_\infty = \text{mes}(D(U, X_0)), \text{ and } b_\infty = \text{mes}(U - X_0).$$

If $\lim_{i \rightarrow \infty} m_i = 0$, then the area U will tend to the set X_0 , i.e., the measure $D(U, X_0)$ will tend to 0. Let us note that the described construction of the model secures $m_{i+1} < m_i$ which, the number of points each of the tests consists of being limited, is equivalent to $m_i \rightarrow 0$. In view of the finite number of lines and points each of the levels can handle, a situ-

ation may occur where we cannot achieve $m_i < m_{i-1}$ at a given level. We then return to the situation which immediately followed the verification during the transition from the level L_{i-1} to the level L_i and we start the new sequence of generalizations $G_{i\mu}^*$. On the other hand, since each of the tests consists in choosing at random a finite number of points, it may happen that for some i $m_{i\mu}^* = 0$, which does not necessarily mean that $D(U, X_0) \approx 0$, where the symbol $A \approx 0$ means that the measure of the set A is 0.

Shown in Fig. 12-16 are some of the consecutive phases of the automaton model operation. Under each of the figures information is given as to the level and the consecutive number of the process of generalization, following which the diagram was made, and the ratios $m_{i\mu}$ and $b_{i\mu}$. Between the phases presented in Fig. 15 and 16 a return to the beginning of the level L_3 took place. The authors have been unable to establish the area X by analytical methods and so the periodic solution of equations (3.1) (without perturbations) was plotted to serve as a "comparison module".

As soon as one of the numbers m_i satisfies the condition $m_i < m_{crit}$, where m_{crit} is a number set in advance, one can, with the aid of the automaton model and proceeding as in Chapter One, determine whether the random trajectory starting from the predetermined point P will remain in the set K . This may be achieved in a considerably shorter time than the performance of even one numerical integration.

The probability of committing an error does not exceed the value m_{crit} .

Conclusion

The relatively small precision of the achieved results indicates that the principal factor which limits the applicability of the described model is the fairly small computing power of the applied computer.

REFERENCES

- [1] Turski W., *Algorytmy*, 1963, S. 1-21.
- [2] Turski W., *Computatio*, 1964, Vol. 1, No. 1, 57-71.
- [3] Ralston A., Wilf H. S., *Mathematical Methods for Digital Computers*. John Wiley and Sons, New York-London, 1962.
- [4] Cesari L., *Asymptotic Behavior and Stability Problems in Ordinary Differential Equations*. Springer-Verlag, Berlin-Göttingen-Heidelberg, 1963.
- [5] Birnbaum Z. W., *Introduction to Probability and Mathematical Statistics*. Harper and Brothers, New York, 1962.
- [6] Urabe M., *Trudy meždunarodnogo simpoziuma po nelineynym kolebanyam*, 1963, Vol. 2, 367 pp.